Light scattering by dielectric bodies in the Born approximation

A. S. Bereza,[1,2] A. V. Nemykin,[1,2] S. V. Perminov,[3] L. L. Frumin,[1,2] and D. A. Shapiro[1,2,*]

[1]*Institute of Automation and Electrometry, Russian Academy of Sciences, Siberian Branch, 1 Koptjug Avenue, Novosibirsk 630090, Russia*

[2]*Novosibirsk State University, 2 Pirogov Street, Novosibirsk 630090, Russia*

[3]*Rzhanov Institute of Semiconductor Physics, Russian Academy of Sciences, Siberian Branch, 13 Lavrent'yev Avenue, Novosibirsk 630090, Russia*

(Received 23 April 2017; published 23 June 2017)

Light scattering is one of the most important elementary processes in near-field optics. We build up the Born series for scattering by dielectric bodies with sharp boundaries. The Green's function for a two-dimensional homogeneous dielectric cylinder is obtained. As an example, the formulas are derived for a scattered field of two parallel cylinders. The polar diagram is shown to agree with the numerical calculation by the known methods of discrete dipoles and boundary elements.

DOI: 10.1103/PhysRevA.95.063839

I. INTRODUCTION

In the past decades substantial progress has been achieved in nano-optics [1–3]. However, a significant methodological deficiency still persists even for basic problems, like scattering by nanosized bodies. Unlike "macroscopic" optics, where transverse waves (for instance, plane or spherical) are very useful to study, say, diffraction and interference, in the subwavelength region the treatment of these phenomena becomes much more complicated. The reason is evanescent waves near the boundary of illuminated objects. Such waves usually can be neglected in optical processes with large scatterers, but in nano-optics this is not the case. Strong coupling via evanescent waves is the key feature that most practical nanophotonics tasks focus on. They include a light energy concentration within a few-nanometer range [4], high-efficiency broad-band solar cells [5], light-induced forces at the nanoscale [6,7], surface-enhanced Raman spectroscopy [8], and the tomographic reconstruction of a nanostructure [9].

Only a few problems allow analytical solutions in photonics. Along with the classical papers on one cylinder [10,11], the scattering from two cylinders [12] and two perfectly conducting spheres [13] can be found in the quasistatic limit using bipolar coordinates; a perfectly conducting cylinder near a surface was considered in terms of cylindrical wave expansion [14]. In more complicated cases, numerical or semianalytical methods become the only ones capable of calculating electromagnetic fields in both near and far regions, for instance, in a system of several cylinders or a periodic chain of them [15–17].

Analytical approximations are very useful for understanding the scattering properties of a structure, at least for testing numerical methods. There is a universal method to derive the formulas based on the Born approximation. It consists in taking the incident field in place of the total field at each point inside the scattering potential. If the scatterer is not sufficiently weak, the next approximations are exploited. Several recent optical research studies have been devoted to high-order terms of the approximation. In optical diffusion tomography high orders are necessary for solving the nonlinear inverse problem [18]. The second-order approximation is needed for numerical reconstruction of a shallow buried object by the scattered amplitude [19]. The resonant-state expansion approximation uses second-order terms to find eigenfrequencies in an optical fiber waveguide [20]. However, the traditional Born series is not applicable to a system of dielectric bodies with sharp edges, as it does not satisfy the boundary conditions.

The main goal of the present work is to construct a modified Born approximation for a set of dielectric bodies. The integral relations are derived and the series for two dielectric cylinders is obtained. We managed to account for the first cylinder exactly by means of the special Green's function for a cylindrical dielectric, which intrinsically includes multiple scattering processes with this cylinder. Thus, another aim of our paper is to derive that special Green's function.

The Born series is constructed in Sec. II. Scattering by two cylinders, considered in Sec. III, illustrates the application of the developed approach. The obtained formulas are in agreement with numerical calculations using surface integral equations and the discrete dipole approximation (DDA). The Green's function is derived in Appendix A: the expressions for a source point inside and outside the dielectric are given for the cases of both p and s waves. The boundary element method (BEM) has been discussed in our works [21–23] devoted to the scattering by cylinders on a dielectric substrate. The formulas for the two-dimensional discrete dipole method are derived in Appendix B.

II. BORN SERIES

The Helmholtz equations for magnetic fields inside and outside the dielectric (denoted by the subscripts "in" and "out," respectively) are

$$\left(\Delta + k_1^2\right)\mathcal{H}_{\text{in}}(\mathbf{r}) = 0, \quad \left(\Delta + k_0^2\right)\mathcal{H}_{\text{out}}(\mathbf{r}) = 0, \tag{1}$$

where Δ is the two-dimensional Laplace operator with respect to the x and y variables, wave numbers $k_0 = \omega/c$ and $k_1 = \sqrt{\varepsilon}\omega/c$, c is the speed of light, ω is the frequency, and ε is the dielectric permittivity. The field $\mathcal{H}_{\text{out}}$ in free space is slightly changed due to a weak perturbation, which is small enough (i.e., $k_1 a \ll 1$, where a is its size) and/or low-polarizable ($|\varepsilon - 1| \ll 1$). The internal field $\mathcal{H}_{\text{in}}$ can be quite different.

*shapiro@iae.nsk.su

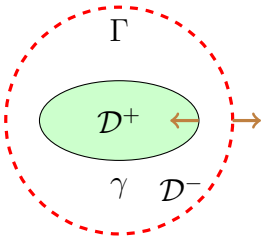

FIG. 1. Domains of integration $\mathcal{D}^+$ and $\mathcal{D}^-$ for Eq. (3). The boundary of $\mathcal{D}^-$ consists of $\gamma = \partial\mathcal{D}^+$ (solid line) and the external infinitely remote contour Γ (dashed line). Arrows indicate external normals $\mathbf{n}$ to $\partial\mathcal{D}^-$.

The Green's function obeys the equation

$$(\Delta + k^2)G = \delta(\mathbf{r} - \mathbf{r}'). \tag{2}$$

Here k is the corresponding value: $k = k_0$ or $k = k_1$.

We use Eqs. (1) and (2) to derive the relations between amplitudes at the boundary:

$$\mathcal{H}_{\text{in}}(\mathbf{r}) = \int_{\mathcal{D}^+} [\mathcal{H}_{\text{in}}(\mathbf{r}')\Delta G_p - G_p \Delta\mathcal{H}_{\text{in}}(\mathbf{r}')]dS',$$
$$\mathcal{H}_{\text{out}}(\mathbf{r}) = \int_{\mathcal{D}^-} [\mathcal{H}_{\text{out}}(\mathbf{r}')\Delta G - G\Delta\mathcal{H}_{\text{out}}(\mathbf{r}')]dS', \tag{3}$$

where dS' is the element of integration over the dielectric domain $\mathcal{D}^+$ or free-space domain $\mathcal{D}^-$ (Fig. 1). The Green's function $G(\mathbf{r},\mathbf{r}')$ describes free space, and $G_p(\mathbf{r},\mathbf{r}')$ is a similar function that corresponds to a dielectric with permittivity ε. The Green's function of free space is the solution of Eq. (2) with $k = k_0$ and can be written as

$$G(\mathbf{r},\mathbf{r}') = \frac{1}{4i}H_0^{(1)}(k|\mathbf{r} - \mathbf{r}'|)$$
$$= \frac{1}{4i}\sum_{m=-\infty}^{\infty} e^{im(\varphi-\varphi')}\begin{cases} H_m^{(1)}(kr\,)J_m(kr'), & r\ > r', \\ H_m^{(1)}(kr')J_m(kr\,), & r' > r\ , \end{cases} \tag{4}$$

where J_m, and $H_m^{(1)}$ are Bessel and Hankel functions [24].

The boundary conditions are

$$\mathcal{H}_{\text{in}}|_\gamma = \mathcal{H}_{\text{out}}|_\gamma, \quad \frac{1}{\varepsilon}\frac{\partial\mathcal{H}_{\text{in}}}{\partial r}\bigg|_\gamma = \frac{\partial\mathcal{H}_{\text{out}}}{\partial r}\bigg|_\gamma, \tag{5}$$

where γ is the contour separating the $\mathcal{D}^-$ and $\mathcal{D}^+$ domains. Applying Green's theorem [25] to Eq. (3) we can reduce the surface integral as

$$\mathcal{H}_{\text{in}}(\mathbf{r}) = \int_\gamma \mathbf{n}[\mathcal{H}_{\text{out}}(\mathbf{r}')\nabla G_p - \varepsilon G_p \nabla\mathcal{H}_{\text{out}}(\mathbf{r}')]dl',$$
$$\mathcal{H}_{\text{out}}(\mathbf{r}) = -\int_\gamma \mathbf{n}\left[\mathcal{H}_{\text{in}}(\mathbf{r}')\nabla G - \frac{1}{\varepsilon}G\nabla\mathcal{H}_{\text{in}}(\mathbf{r}')\right]dl'$$
$$+ \int_\Gamma \mathbf{n}[\mathcal{H}_{\text{out}}(\mathbf{r}')\nabla G - G\nabla\mathcal{H}_{\text{out}}(\mathbf{r}')]dl', \tag{6}$$

where dl' is the element of path, $\mathbf{n}$ is the unit vector along the external normal, and Γ is some remote contour (Fig. 1).

The integral over Γ can be calculated explicitly by the known relation for the Wronskian determinant [24]:

$$-\frac{k\rho}{4i}\int_{-\pi}^{\pi}\left[H_0^{(1)}(k\rho) + i\cos\varphi H_1^{(1)}(k\rho)\right]e^{ik\rho\cos\varphi}\,d\varphi$$
$$= 2\pi k\rho\left[J_1(k\rho)H_0^{(1)}(k\rho) - J_0(k\rho)H_1^{(1)}(k\rho)\right] = 1.$$

Then this integral reproduces the field of a plane incident wave $\mathcal{H}_{\text{out}}^{(0)} = \mathcal{H}_0 e^{i\mathbf{kr}}$. Equations (6) are similar to boundary integral equations; the only difference is the absence of the factor $1/2$ in the terms outside the integral. These terms are given within the external or internal limit, in contrast to boundary equations, where they are determined directly at the contour [26].

The successive approximation series can be built up for both external and internal fields:

$$\mathcal{H}_{\text{out}} = \mathcal{H}_{\text{out}}^{(0)} + \mathcal{H}_{\text{out}}^{(1)} + \cdots, \quad \mathcal{H}_{\text{in}} = \mathcal{H}_{\text{in}}^{(0)} + \mathcal{H}_{\text{in}}^{(1)} + \cdots. \tag{7}$$

Then from (6) we get the recurrent relations:

$$\mathcal{H}_{\text{in}}^{(j)}(\mathbf{r}) = \int_\gamma \mathbf{n}\left[\mathcal{H}_{\text{out}}^{(j)}(\mathbf{r}')\nabla G_p - \varepsilon G_p \nabla\mathcal{H}_{\text{out}}^{(j)}(\mathbf{r}')\right]dl',$$
$$\mathcal{H}_{\text{out}}^{(j+1)}(\mathbf{r}) = \int_\gamma \mathbf{n}\left[\frac{G}{\varepsilon}\nabla\mathcal{H}_{\text{in}}^{(j)}(\mathbf{r}') - \mathcal{H}_{\text{in}}^{(j)}(\mathbf{r}')\nabla G\right]dl'. \tag{8}$$

The approximation exactly takes into account the boundary conditions, what is distinct from the Born approach in quantum mechanics. This is to emphasize that the shape of the contour γ can be arbitrary; the circular cylinder (considered in the next section) is, basically, just the simplest example. The dielectric region $\mathcal{D}^-$ could be unconnected; in that case the contour γ is the sum of all the boundaries of dielectric domains.

III. SCATTERING BY TWO CYLINDERS

Let us now consider two cylinders (see Fig. 2). There are three domains, with different dielectric permittivities. The Helmholtz equation (2), is valid for $k_0 = \omega/c$, $k_1 = \sqrt{\varepsilon}\omega/c$,

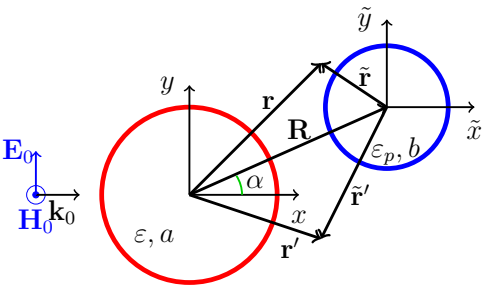

FIG. 2. Scheme of p-wave scattering by two parallel cylinders. The dielectric permittivity and the radius are indicated in the first (left) and second (right) cylinders. The external infinitely remote contour Γ is not shown.

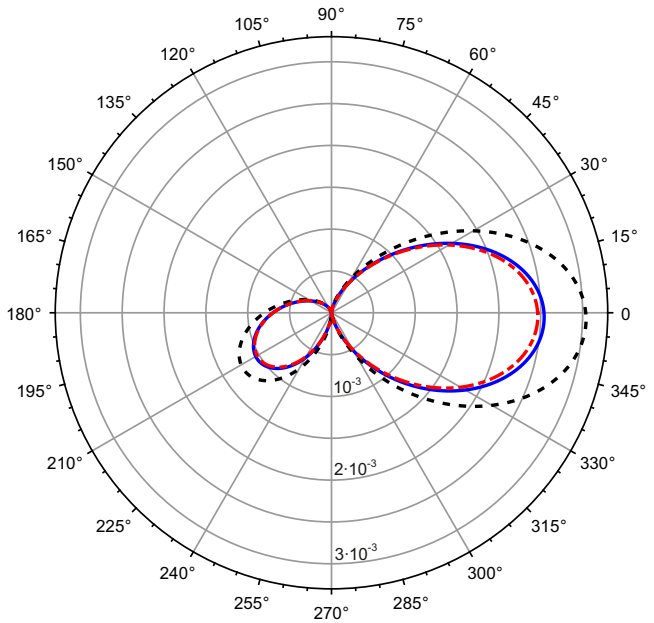

FIG. 3. Polar diagram of scattering by a pair of equal dielectric cylinders at $a = b = 0.1$ μm, $\varepsilon_p = \varepsilon = 2.25$, and $R = 0.3$ μm at incidence angle $\alpha = -\pi/4$, wavelength $\lambda = 1.5$ μm, and distance between the observation point and the center of the first cylinder $r = 2\lambda$. First Born approximation (dotted line), second Born approximation (dashed line), and BEM (solid line).

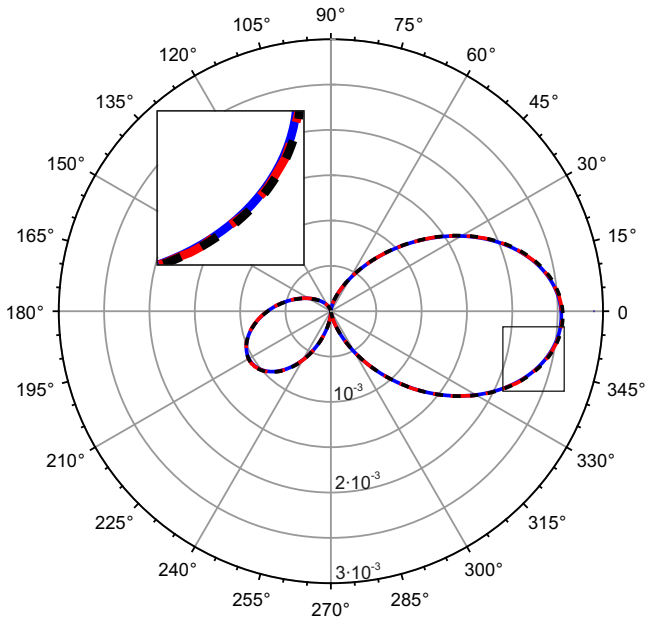

FIG. 4. Polar diagram of the scattered field with the same parameters as in Fig. 3: third Born approximation (dotted line), BEM (solid line), and DDA (dashed line). Inset: Magnifcation of the area of the main plot indicated by the box.

or $k_p = \sqrt{\varepsilon_p}\omega/c$, and condition (5) is

$$\mathcal{H}_{\rm in}|_\gamma = \mathcal{H}_{\rm out}|_\gamma, \quad \frac{1}{\varepsilon}\frac{\partial \mathcal{H}_{\rm in}}{\partial r}\bigg|_\gamma = \frac{\partial \mathcal{H}_{\rm out}}{\partial r}\bigg|_\gamma,$$
$$\mathcal{H}_p|_{\gamma_p} = \mathcal{H}_{\rm out}|_{\gamma_p}, \quad \frac{1}{\varepsilon_p}\frac{\partial \mathcal{H}_p}{\partial \tilde{r}}\bigg|_{\gamma_p} = \frac{\partial \mathcal{H}_{\rm out}}{\partial \tilde{r}}\bigg|_{\gamma_p}. \qquad (9)$$

We treat the second cylinder as the perturbation here. Let us obtain a number of successive approximations for the whole complicated configuration shown in Fig. 2. We exploit the Green's function for cylindric geometry (A12). Using this function makes it possible to account for the first cylinder exactly including the multiple scattering. The second cylinder is described in terms of the Born approximation. To find the number of terms sufficient to get the field with a given accuracy, we compare it with numerical solutions obtained by known well-studied approaches, namely, the discrete dipole approximation and boundary element methods.

The boundary equations are analogous to (6). When the perturbation is weak, expansion (7) yields

$$\mathcal{H}_p^{(j)}(\tilde{\mathbf{r}}) = \int_{\gamma_p} \mathbf{n}\big[\mathcal{H}_{\rm out}^{(j)}(\mathbf{r}')\nabla G_p - \varepsilon_p G_p \nabla \mathcal{H}_{\rm out}^{(j)}(\mathbf{r}')\big]d\tilde{l}',$$
$$\mathcal{H}_{\rm out}^{(j+1)}(\mathbf{r}) = \int_{\gamma_p} \mathbf{n}\left[\frac{G}{\varepsilon_p}\nabla \mathcal{H}_p^{(j)}(\tilde{\mathbf{r}}') - \mathcal{H}_p^{(j)}(\tilde{\mathbf{r}}')\nabla G\right]d\tilde{l}'. \qquad (10)$$

Here $G_p = G_p(\tilde{\mathbf{r}},\tilde{\mathbf{r}}')$, $\tilde{\mathbf{r}} = \mathbf{r} - \mathbf{R}$, $\mathbf{n} = \mathbf{n}_{\gamma_p}$. The recurrence relations are valid for arbitrary shape of the perturber with a sharp boundary, provided its layout is in the external region of the main cylinder. The integral over the boundary of the perturber can be calculated. The final relation is a Fourier series in azimuthal angle with a shift due to the axis offset. The coefficients of series are:

$$D_p^{m(0)} = \frac{\pi k_p b}{2i}[J_m(k_0 b)H_m'(k_p b) - \sqrt{\varepsilon_p}J_m'(k_0 b)H_m(k_p b)]\left[i^m e^{ik_0 R\cos\alpha} + \sum_{n=-\infty}^{\infty} i^n e^{i(n-m)\alpha} C_n H_{n-m}(k_0 R)\right],$$

$$D_p^{m(j)} = \frac{\pi k_p b}{2i}\left\{\tilde{D}_{\rm out}^{m(j)}[H_m(k_0 b)H_m'(k_p b) - \sqrt{\varepsilon_p}H_m'(k_0 b)H_m(k_p b)]\right.$$
$$\left. + \sum_{n=-\infty}^{\infty} D_{\rm out}^{n(j)} e^{i(n-m)\alpha} H_{n-m}(k_0 R)[J_m(k_0 b)H_m'(k_p b) - \sqrt{\varepsilon_p}J_m'(k_0 b)H_m(k_p b)]\right\},$$

$$D_{\rm out}^{m(j+1)} = -\frac{\pi k_0 b}{2i} C_m \sum_{n=-\infty}^{\infty} D_p^{n(j)} e^{i(n-m)\alpha} H_{m-n}(k_0 R)\left[J_n(k_p b)J_n'(k_0 b) - \frac{1}{\sqrt{\varepsilon_p}}J_n'(k_p b)J_n(k_0 b)\right],$$

$$\tilde{D}_{\rm out}^{m(j+1)} = -\frac{\pi k_0 b}{2i} D_p^{m(j)}\left[J_m(k_p b)J_m'(k_0 b) - \frac{1}{\sqrt{\varepsilon_p}}J_m'(k_p b)J_m(k_0 b)\right].$$

Hereafter the upper index (1) of the Hankel function is omitted; the prime indicates the derivative of a cylindric function with respect to its argument.

Figure 3 shows the angular dependence of the scattered field square $|\mathcal{H}_{sc}/\mathcal{H}_0|^2$. As the figure demonstrates, the first approximation gives a rather correct qualitative description of the diagram, with a deviation of 15%. The error of the second order is nearly 3%. Figure 4 shows the comparison of the third Born approximation with calculations by the BEM and DDA. The deviation appears to be about 1%.

IV. CONCLUSIONS

The Green's function for a dielectric cylinder is found in the cases of p and s waves with source points inside and outside the cylinder. High-order Born approximations of two dielectrics with sharp boundaries are reduced to recurrence relations. This technique is analytically applied to the scattering by a pair of cylinders. The first approximation demonstrates its qualitative agreement in shape with numerical results. The second and third approximations are shown to agree quantitatively with calculations by boundary elements and discrete dipoles.

ACKNOWLEDGMENTS

The authors are grateful to O. V. Belai for helpful discussions. This work was supported by the Russian Foundation for Basic Research (16-02-00511) and the Council for grants of President of Russian Federation (NSh-6898.2016.2).

APPENDIX A: SCALAR GREEN'S FUNCTION

Let us consider a cylinder whose axis is along the z direction, as shown in Fig. 5. We are looking for the scalar Green's function $G(\mathbf{r},\mathbf{r}')$, which is the solution to the inhomogeneous two-dimensional Helmholtz equation (2), with $k = k_0$ in free space and $k = k_1$ in the dielectric.

Rewrite the delta function (2), in polar coordinates,

$$\delta(\mathbf{r}-\mathbf{r}') = \frac{1}{r}\delta(r-r')\delta(\varphi-\varphi'), \tag{A1}$$

where r, φ and r',φ' are the polar coordinates of the source and observation points and decompose the angular factor into the Fourier series:

$$\delta(\varphi-\varphi') = \frac{1}{2\pi}\sum_{m=-\infty}^{\infty} e^{im(\varphi-\varphi')}. \tag{A2}$$

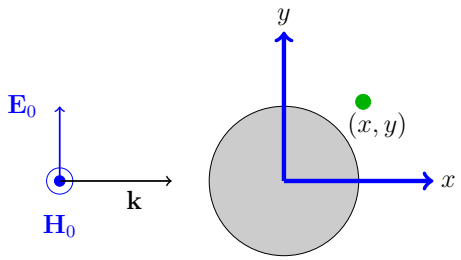

FIG. 5. Right: Cross section of an infinite cylinder in homogeneous space. The green circle indicates the observation point $\mathbf{r} = (x,y)$. Left: p polarization.

The coefficient $1/2\pi$ is found from the delta-function normalization $\int_{-\pi}^{\pi}\delta(\varphi)\,d\varphi = 1$.

Expanding the Green's function in partial waves

$$G(r,\varphi;r',\varphi') = \sum_{m=-\infty}^{\infty} g_m(r,r')e^{im(\varphi-\varphi')} \tag{A3}$$

and substituting into (2), we get an ordinary equation for each m:

$$\frac{d^2g_m}{dr^2} + \frac{1}{r}\frac{dg_m}{dr} + \left(k^2 - \frac{m^2}{r^2}\right)g_m = \frac{1}{2\pi r}\delta(r-r'). \tag{A4}$$

At $r > r'$ or $r < r'$, the corresponding solutions can be expressed through the combinations of Bessel and Hankel functions, $k = k_0$:

$$g_m = \begin{cases} a_m J_m(k_1 r), & r < a, \\ A_m J_m(kr) + B_m H_m(kr), & a < r < r', \\ d_m H_m(kr), & r' < r. \end{cases} \tag{A5}$$

Conditions (5) are the continuity of the magnetic field and its weighted normal derivative at the interface between dielectric and free space, $r = a$,

$$[g_m]_{r=a} = 0, \quad \left[\frac{1}{\varepsilon}\frac{dg_m}{dr}\right]_{r=a} = 0, \tag{A6}$$

where the brackets denote a jump of the corresponding value. The conditions are written for a p wave, where the magnetic field is parallel to the z axis. The next pair of conditions follows from the continuity of the Green's function and the jump of its first derivative at $r = r'$:

$$[g_m]_{r=r'} = 0, \quad \left[\frac{dg_m}{dr}\right]_{r=r'} = \frac{1}{2\pi r'}. \tag{A7}$$

We omit the Hankel function in the first line and Bessel function in the third line in Eq. (A5) on the basis of regularity at $r \to 0$ and the Sommerfeld radiation requirement at $r \to \infty$.

Substituting (A5) into boundary conditions (A6) and (A7) we get the set for the coefficients:

$$A_m J_m(ka) + B_m H_m(ka) = a_m J_m(k_1 a), \tag{A8}$$

$$\begin{aligned} A_m J'_m(ka) + B_m H'_m(ka) &= \frac{1}{\sqrt{\varepsilon}} a_m J'_m(k_1 a), \\ A_m J_m(kr') + B_m H_m(kr') &= d_m H_m(kr'), \\ A_m J'_m(kr') + B_m H'_m(kr') &= d_m H'_m(kr') - \frac{1}{2\pi kr'}. \end{aligned} \tag{A9}$$

From (A8) we get $B_m = \alpha_m A_m$, where

$$\alpha_m = \frac{J_m(ka)J'_m(k_1 a) - \sqrt{\varepsilon}J'_m(ka)J_m(k_1 a)}{\sqrt{\varepsilon}H'_m(ka)J_m(k_1 a) - H_m(ka)J'_m(k_1 a)}. \tag{A10}$$

Then the determinant of the set (A9), for coefficients A_m and d_m is $\{J_m + \alpha_m H_m, H_m\} = 2i/\pi kr'$, where the curly bracket stands for the Wronskian $\{f,g\} = fg' - f'g$ at $r = r'$.

Let us summarize the formulas for the partial Green's function. At $r' < a$ they are

$$g_m = \begin{cases} \frac{1}{4i} J_m(k_1 r\,) Z_1(k_1 r'), & 0 < r < r', \\ \frac{1}{4i} J_m(k_1 r') Z_1(k_1 r), & r' < r < a, \\ \beta_m H_m(k_0 r) J_m(k_1 r'), & a < r, \end{cases}$$

$$C_m = -\frac{H_m(k_1 a) H'_m(k_0 a) - \varepsilon^{\nu} H'_m(k_1 a) H_m(k_0 a)}{\Delta}, \quad \text{(A11)}$$

where $Z_1(z) = C_m J_m(z) + H_m(z)$, $\beta_m = \varepsilon^{\nu}/2\pi k_1 a \Delta$.

At $r' > a$ the formulas are

$$g_m = \begin{cases} \beta_m J_m(k_1 r\,) H_m(k_0 r'), & r < a, \\ \frac{1}{4i} H_m(k_0 r') Z_2(k_0 r), & a < r < r', \\ \frac{1}{4i} H_m(k_0 r\,) Z_2(k_0 r'), & a < r' < r, \end{cases}$$

$$C_m = -\frac{J_m(k_1 a) J'_m(k_0 a) - \varepsilon^{\nu} J'_m(k_1 a) J_m(k_0 a)}{\Delta}, \quad \text{(A12)}$$

$$\Delta = J_m(k_1 a) H'_m(k_0 a) - \varepsilon^{\nu} J'_m(k_1 a) H_m(k_0 a),$$

where $Z_2(z) = J_m(z) + C_m H_m(z)$, $\beta_m = 1/2\pi k_0 a \Delta$. The formulas with $\nu = -1/2, 1/2$ refer to the case of p and s waves, respectively.

APPENDIX B: DDA

Below we briefly recall the two-dimensional DDA approach [27] to obtain the particular relationships we used in our calculations. Let us have some scattering body, with volume V (which is per unit length along the z direction in the two-dimensional case) and permittivity ε (which is constant within the body), placed in vacuum. From the Helmholtz equation we obtain the integral equation for an isotropic medium,

$$\mathbf{E}(\mathbf{r}) = \mathbf{E}_{\rm inc}(\mathbf{r}) + \int_{V \setminus V_0} d^2 r' [\widehat{\mathbf{G}}(\mathbf{r},\mathbf{r}') \chi(\mathbf{r}') \mathbf{E}(\mathbf{r}')] + \int_{V_0} d^2 r' [\widehat{\mathbf{G}}(\mathbf{r},\mathbf{r}') \chi(\mathbf{r}') \mathbf{E}(\mathbf{r}')], \quad \text{(B1)}$$

where V_0 is a small volume around the singularity point $\mathbf{R} = \mathbf{r} - \mathbf{r}' \to 0$, $V \setminus V_0$ is the volume of the dielectric without the singular part, $\mathbf{E}_{\rm inc}(\mathbf{r})$ is the given field of the incident wave, $\chi(\mathbf{r}) \equiv (\varepsilon - 1)/4\pi$ is the polarizability, and the Green's tensor $\widehat{\mathbf{G}}(\mathbf{r},\mathbf{r}')$ is the solution to the Maxwell equations:

$$\mathrm{rot}\,\mathrm{rot}\,\widehat{\mathbf{G}} - k^2 \widehat{\mathbf{G}} = 4\pi k^2 \delta(\mathbf{r} - \mathbf{r}'). \quad \text{(B2)}$$

The Green's tensor obeying (B2) can be expressed [1,26] in terms of the scalar Green's function g, which satisfies Eq. (2),

$$G_{\alpha\beta} = 4\pi \left(k^2 \delta_{\alpha\beta} + \nabla_\alpha \nabla_\beta\right) g, \quad \text{(B3)}$$

where α and β are Cartesian indices. Then, it is well known that the Green's tensor actually depends on the difference $\mathbf{R}$. Finally, in the two-dimensional case we have

$$G_{\alpha\beta}(\mathbf{R}) = \frac{i\pi k}{R}\left[A(kR)\delta_{\alpha\beta} - B(kR)\frac{R_\alpha R_\beta}{R^2}\right], \quad A(x) = x H_0(x) - H_1(x), \quad B(x) = x H_0(x) - 2H_1(x), \quad \text{(B4)}$$

where $\mathbf{R} = \mathbf{r} - \mathbf{r}'$, $H_0(x)$, $H_1(x)$ are Hankel functions of the first kind.

In Eq. (B1) we implicitly isolate the term that includes the singularity of the Green's tensor at $\mathbf{r} = \mathbf{r}'$ by means of a small volume V_0, for which the point $\mathbf{r}$ is internal. Then we rewrite this term, introducing the following quantities:

$$\widehat{\mathbf{M}}(V_0,\mathbf{r}) = \int_{V_0} d^2 r' \left[G_{\alpha\beta}(\mathbf{r} - \mathbf{r}') - \frac{4R_\alpha R_\beta - 2\delta_{\alpha\beta} R^2}{R^4}\right] \chi(\mathbf{r}') \mathbf{E}(\mathbf{r}') \quad \text{(B5)}$$

and

$$\widehat{\mathbf{L}}(V_0,\mathbf{r}) = -\int_{V_0} d^2 r' \frac{4R_\alpha R_\beta - 2\delta_{\alpha\beta} R^2}{R^4} \chi(\mathbf{r}') \mathbf{E}(\mathbf{r}'). \quad \text{(B6)}$$

Note that $\widehat{\mathbf{M}}$ is free from the singularity, thus $\widehat{\mathbf{M}} \to 0$ with $V_0 \to 0$. The fraction under integration is, basically, the static limit (at $k \to 0$) of the Green's tensor. Also, we need to discretize the whole scattering volume V into parts V_j (in such a way that V_0 coincides with one of them). With the use of (B5) and (B6), Eq. (B1) becomes

$$\mathbf{E}(\mathbf{r}_i) = \mathbf{E}_{\rm inc}(\mathbf{r}_i) + \sum_{j \neq i} \int_{V_j} d^2 r' [\widehat{\mathbf{G}}(\mathbf{r}_i - \mathbf{r}') \chi(\mathbf{r}') \mathbf{E}(\mathbf{r}')] + \widehat{\mathbf{M}}(V_i,\mathbf{r}_i) - \widehat{\mathbf{L}}(V_i,\mathbf{r}_i), \quad \text{(B7)}$$

where $\mathbf{r}_i$ denotes a point lying inside the volume V_i.

Up to this line, the equations are fully correct as exact consequences of the initial wave equation. Now we make two approximations: the first is that $\mathbf{E}(\mathbf{r}')$ and $\chi(\mathbf{r}')$ are constant within the volume V_j; the second approximation assumes that

$$\frac{1}{V_j} \int_{V_j} d^2 r' \widehat{\mathbf{G}}(\mathbf{r}_i,\mathbf{r}') = \widehat{\mathbf{G}}(\mathbf{r}_i,\mathbf{r}_j). \quad \text{(B8)}$$

Condition (B8) is intrinsically contained in all DDA formulations [28], which initially deal with replacing the scatterer with a set of point dipoles. If the volumes V_i are square cells (we should keep in mind that we are treating the two-dimensional case), then we can place the points $\mathbf{r}_i$ in the center of the corresponding squares.

Below, we neglect $\widehat{\mathbf{M}}$, as most authors do, thus choosing the simpler (or "weak") DDA formulation [28,29]. Integrating (B6) we transform (B7) into its final form,

$$\mathbf{d}_i \widehat{\alpha}_i^{-1} = \mathbf{E}_{i,\rm inc} + \sum_{j \neq i} \widehat{\mathbf{G}}(\mathbf{r}_i - \mathbf{r}_j) \mathbf{d}_j, \quad \text{(B9)}$$

where we denote, for simplicity, the dependence on $\mathbf{r}_i$ (and $\mathbf{r}_j$) by the corresponding subscript; $\mathbf{d}_i = V_i \chi_i \mathbf{E}_i$ is the polarization of the volume V_i (basically, its dipole moment, as we took χ_i and $\mathbf{E}_i$ to be constant within V_i); and $\widehat{\alpha}_i$ is the polarizability tensor, defined as

$$\widehat{\alpha}_i = \widehat{\mathbf{I}} V_i \chi_i (1 + 2\pi\chi_i)^{-1} \equiv \frac{a^2}{2} \frac{\varepsilon - 1}{\varepsilon + 1} \widehat{\mathbf{I}}. \quad \text{(B10)}$$

The last term is the known quasistatic dipole polarizability of a thin cylinder (two-dimensional dipole) with the cross section πa^2 equal to V_i.

Thus, the calculations consisted in finding the dipole moments $\mathbf{d}_i$ by solving (B9) with (B10) and (B4). From them, all the quantities of interest can be obtained. In our case, we calculate the scattered magnetic field.

[1] L. Novotny and B. Hecht, *Principles of Nano-Optics* (Cambridge University Press, Cambridge, UK, 2006).
[2] C. Girard, Rep. Prog. Phys. **68**, 1883 (2005).
[3] S. Kawata and V. M. Shalaev (eds.), *Nanophotonics with Surface Plasmons* (Elsevier, Oxford, UK, 2007).
[4] M. I. Stockman, Phys. Today **64**, 39 (2011).
[5] S. Y. Chou and D. Wei, Opt. Express **21**, A60 (2013).
[6] S. V. Perminov, V. P. Drachev, and S. G. Rautian, Opt. Lett. **33**, 2998 (2008).
[7] D. Shapiro, D. Nies, O. Belai, M. Wurm, and V. Nesterov, Opt. Express **24**, 15972 (2016).
[8] K. A. Willets and R. P. Van Duyne, Annu. Rev. Phys. Chem. **58**, 267 (2007).
[9] T. Yamaoki, H. Hamada, and O. Matoba, Appl. Opt. **55**, 6874 (2016).
[10] L. Rayleigh, Philos. Mag. Ser. 6 **36**, 365 (1918).
[11] J. R. Wait, Can. J. Phys. **33**, 189 (1955).
[12] P. E. Vorobev, Sov. Phys. JETP **110**, 193 (2010).
[13] I. E. Mazets, Sov. Phys. Tech. Phys. **45**, 1238 (2000).
[14] R. Borghi, F. Frezza, G. Schettini, F. Gori, and M. Santarsiero, J. Opt. Soc. Am. A **13**, 483 (1996).
[15] K. J. Schaudt, N.-H. Kwong, and J. D. Garcia, Phys. Rev. A **44**, 4076 (1991).
[16] S. Belan and S. Vergeles, Opt. Mater. Express **5**, 130 (2015).
[17] S.-C. Lee, J. Quant. Spectrosc. Radiat. Transfer **182**, 119 (2016).
[18] G. Y. Panasyuk, V. A. Markel, P. Scott Carney, and J. C. Schotland, Appl. Phys. Lett. **89**, 221116 (2006).
[19] M. Salucci, G. Oliveri, A. Randazzo, M. Pastorino, and A. Massa, J. Opt. Soc. Am. A **31**, 1167 (2014).
[20] M. B. Doost, Phys. Rev. A **93**, 023835 (2016).
[21] O. V. Belai, L. L. Frumin, S. V. Perminov, and D. A. Shapiro, Opt. Lett. **36**, 954 (2011).
[22] O. V. Belai, L. L. Frumin, S. V. Perminov, and D. A. Shapiro, Europhys. Lett. **97**, 10007 (2012).
[23] L. L. Frumin, A. V. Nemykin, S. V. Perminov, and D. A. Shapiro, J. Opt. **15**, 085002 (2013).
[24] F. W. J. Ovler, D. W. Lozier, R. F. Boisvert, and C. W. Clark, *NIST Handbook of Mathematical Functions* (Cambridge University Press, New York, 2010).
[25] J. D. Jackson, *Classical Electrodynamics* (Wiley, New York, 1999).
[26] A. M. Kern and O. J. F. Martin, J. Opt. Soc. Am. A **26**, 732 (2009).
[27] O. J. F. Martin and N. B. Piller, Phys. Rev. E **58**, 3909 (1998).
[28] M. Yurkin and A. Hoekstra, J. Quant. Spectrosc. Radiat. Transfer **106**, 558 (2007).
[29] A. Lakhtakia, Int. J. Mod. Phys. C **03**, 583 (1992).